Tutorial

Fabrication of planar nanomechanical photonic metamaterials

João Valente

Optoelectronics Research Centre and Centre for Photonic Metamaterials, University of Southampton, SO17 1BJ, UK
School of Engineering, University of Glasgow, G12 8LT, UK

E-mail: joao.valente@glasgow.ac.uk

Abstract.

Metamaterials have been around for almost two decades providing great advances in optics and photonics. Despite many fundamental studies and several predicted applications, only recently metamaterials found niche applications and started being implemented in products available to the consumer. Applications are still limited by the static nature of conventional metamaterials, meaning that the function of a specifically designed metamaterial cannot be changed after fabrication. For example, a metamaterial which is designed to absorb at a certain wavelength would become far more useful if it could shift its absorption peak in response to an external control signal. A promising way of overcoming this design limitation is through exploitation of planar nanomechanical photonic metamaterials. Structurally reconfigurable photonic metamaterials based on dielectric membranes of nanoscale thickness provide a simple platform for achieving high levels of modulation contrast and modulation frequency. These metamaterial systems can provide tuneable optical properties arising from nanomechanical displacements driven externally through different mechanisms. Using different actuation forces and designs, tunable devices able to change their transmission, absorption or reflection characteristics can be attained. In this tutorial, we will focus on planar nanomechanical photonic metamaterials while acknowledging considerable work developed using other tuneable metamaterials platfomrs, such as bulk, 3D or multilayer reconfigurable metamaterials. Planar reconfigurable photonic metamaterials are reviewed, nanoactuation mechanisms are explained, nanofabrication processes discussed and some conclusions on future challenges are drawn. Planar nanomechanical photonic metamaterials and their tuneable optical properties can become powerful components for optical devices, optical circuitry and introduce themselves to novel applications.

Keywords: Planar nanomechanical photonic metamaterials, Optical NEMS, Tuneable metamaterials, Nanofabrication

Submitted to: *J. Opt.*

1. Introduction

Engineering of optical materials has generated huge scientific progress with enormous impact in our economy and society, for example, the fiber optic communication network powering the internet, optical data storage and lasers. However, natural media are reaching their limits (i.e. diffraction limit or positive refractive index) affecting our ability to progress further. Metamaterials offer solutions for overcoming some, if not all, of these physical limitations [1–7].

Metamaterials are a young class of structurally engineered materials or composites, which has enabled striking developments in electromagnetic wave control and manipulation [8]. Metamaterials open up the possibility of attaining electromagnetic responses not found in natural media [1, 2], enhancing natural electromagnetic effects [9] and achieving control over light-matter interactions [4]. Manipulation of electromagnetic waves at will can be achieved by engineering the effective electromagnetic parameters of the metamaterial so that the electromagnetic wave perceives the metamaterial as an effectively homogeneous media. Control over such metamaterials parameters, i.e. the permittivity (ϵ_{eff}) and permeability (μ_{eff}), can be obtained through careful design and manufacturing of sub-wavelength size metamolecules (artificial metamaterial 'atoms'). In order to interact as an effective homogeneous medium with visible and near infrared wavelengths, the metamolecules that make up the metamaterial must be smaller than the relevant optical wavelength of hundreds of nanometers, with typical features on the nanometer scale. Moreover, reconfiguring and tuning optical properties of such optical metamaterials will require practical and simple ways of changing size/structure of the metamolecules. Dynamic control over metamaterials optical properties is the main topic of this tutorial manuscript. Several approaches to the subject of metamaterials tuneability have been explored and reported in literature. Bulk and multilayer tuneability using microwave and RF metamaterials [10, 11], multilayer tuneable metamaterials for Terahertz radiation [12, 13] or reconfigurable membranes on top of a substrate for mid and near IR wavelengths [14, 15] are just some examples how to achieve tuneable properties with metamaterials, a extensive review was written by Turpin *et al.* [16]. Here we will give special focus on a novel concept, known as planar reconfigurable photonic metamaterials, that allows control of the interaction of planar metamaterials with infrared and visible light. Taking advantage of well-established silicon-based nanofabrication technologies and by using externally-controlled forces between elastic elements of the metamaterial nanostructure, dynamic control over the optical properties of planar photonic metamaterials can be achieved.

In this tutorial, planar reconfigurable photonic metamaterials physics and nanofabrication will be explained and discussed. From careful metamolecule design to optimization of fabrication processes, this tutorial intends to give details and help others with the development of metamaterial devices for real-world applications. Tuning metamaterials optical properties at infrared and visible wavelengths in a way that is practical for implementation into metadevices will open up a range of applications in telecommunications and stealth technology.

1.1. Controlling light with nanomechanical photonic metamaterials

A metamaterial derives its optical interaction properties from the man-made unit cells of subwavelength size that it consists of. Placed in arrays, the characteristics of these tiny metamolecules will combine in such a way that a homogeneous (non-diffracting) electromagnetic response can be attributed to the resultant metamaterial.

Nanomechanical photonic metamaterials are, usually, assembled from just slightly sub-wavelength elements and are very thin compared to the wavelength, which makes the use of homogenized material parameters problematic. When the artificial medium consists of a structured material of deeply sub-wavelength thickness, it becomes the two-dimensional counterpart of a metamaterial, a so-called metasurface or planar metamaterial (Figure 1a). For such surfaces, we cannot assign the usual effective parameters of bulk media, for example, an effective refractive index only has physical meaning when there is a medium to travel through. In such designed surfaces, dimensions of the constituent metamolecules might be deeply sub-wavelength only in one direction and the electromagnetic wave interaction can be described theoretically based on boundary conditions rather than bulk constitutive parameters [17]. This limiting case is best approximated by a single periodically patterned metal layer with a thickness that is comparable to the skin depth, which is the char-

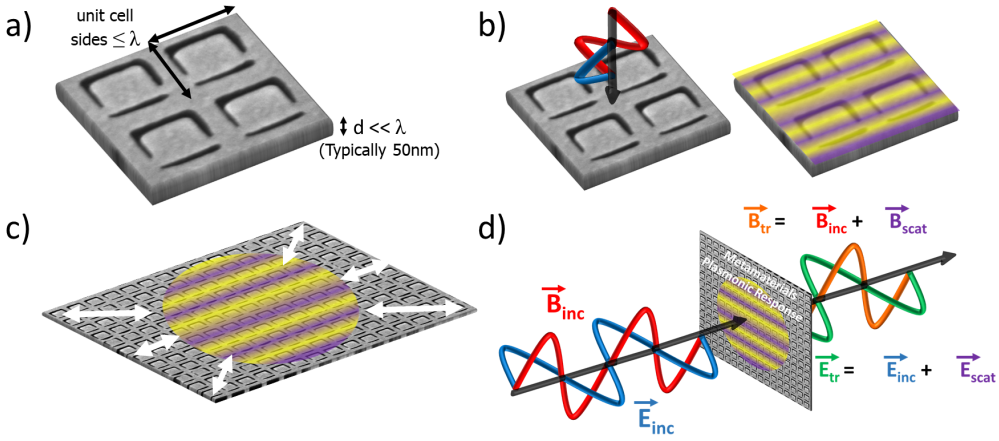

Figure 1. Planar metamaterial optical properties. a) Typical dimensions of a planar photonic metamaterial made of nanostructured gold thin film layer. One of the dimensions must be much smaller than the wavelenght (λ), in this case the thickness, d, is much smaller than the side of the unit cell. b) Plasmonic excitation within the metamolecule by the incident wave - electric field (blue wave), magnetic field (red wave) and plasmonic oscillation (purple and yellow stripes). c) Electromagnetic coupling of metamolecules within the array - expansion of the plasmonic oscillation (purple and yellow stripes). d) Incident wave interaction [electric field (blue wave), magnetic field (red wave)] with a planar metamaterial and resultant transmitted electromagnetic wave: coupling (purple and yellow stripes) and transmission [electric (green wave), magnetic field (orange wave)].

acteristic thickness of the current carrying layer at a conductor's surface.

Such nanostructures, due to their sub-wavelength periodicity, do not diffract electromagnetic waves at normal incidence. The transmission and reflection properties of such planar metamaterials can be written in terms of the transmission (t) and reflection (r) matrices, which relate the transmitted and reflected electric fields, $\vec{E}^t$ and $\vec{E}^r$, to the incident field $\vec{E}^0$. Considering a forward propagating incident wave (indicated by the arrow over the matrix), these relations can be written as,

$$\overrightarrow{E}^t = \overrightarrow{t}\,\overrightarrow{E}^0, \tag{1}$$

$$\overrightarrow{E}^r = \overrightarrow{r}\,\overrightarrow{E}^0. \tag{2}$$

Due to their deeply sub-wavelength thickness, planar metamaterials can be also regarded as a 0 thickness discontinuity which will scatter electromagnetic waves. Therefore, it is convenient to express transmission and reflection in terms of the scattering matrix, s. As a nanomechanical photonic metamaterial is just a non-diffracting array of scatterers, the transmitted field is simply the superposition of the scattered field and the incident wave, as represented by,

$$\overrightarrow{t} = \overrightarrow{s} + 1, \tag{3}$$

where 1 is the unit matrix. Also, these nanomechanical planar photonic metamaterials can only couple to tangential electric fields (along the metamaterial surface) and normal magnetic fields (perpendicluar to the metamaterial surface). Coupling to normal electric fields and tangential magnetic fields is not possible, as the electric charges cannot leave the plane of the structure, see Figure 1. Consequently, two electromagnetic waves that do not differ in the normal (magnetic) and tangencial (electric) field components must excite the photonic metamaterial in the same way. Particularly, the electric field radiated by the photonic metamaterial (or planar current configuration) must be symmetric with respect to the nanostructure. This is why the scattering matrix in the reflection direction differs from the scattering matrix in the transmitted one by a coordinate transformation. The reflection matrix for forward propagating incident waves is,

$$\overrightarrow{r} = \overrightarrow{s}, \tag{4}$$

if the matrices describe normally incident linearly polarized basis states relative to a coordinate system that is fixed to the lab (coordinates do not depend on the wave propagation direction). For a nanomechanical planar photonic metamaterial, transmission and reflection matrices are linked by equation 3 and equation 4. Therefore, nanomechanical planar photonic metamaterials can be described in terms of their scattering properties [18], represented by the scattering matrix of the array of metamolecules, s. The scattering properties for opposite directions of incidence onto a nanomechanical photonic metamaterial are linked by Lorentz reciprocity [19] and therefore the scattering, reflection and transmission matrices for opposite directions of il-

luminations (arrows) take the following form:

$$\overrightarrow{r} = \overrightarrow{s} = \begin{pmatrix} a & b \\ c & d \end{pmatrix} \quad \text{and} \quad \overleftarrow{r} = \overleftarrow{s} = \begin{pmatrix} a & c \\ b & d \end{pmatrix}, \tag{5}$$

$$\overrightarrow{t} = \begin{pmatrix} a+1 & b \\ c & d+1 \end{pmatrix} \quad \text{and} \quad \overleftarrow{t} = \begin{pmatrix} a+1 & c \\ b & d+1 \end{pmatrix}. \tag{6}$$

Upon interference of the incident electromagnetic wave with the scattered field, a new transmitted electromagnetic wave shape in terms of intensity, phase and polarization is produced.

The electromagnetic response of planar metamaterials is controlled by plasmonic excitations within the metamolecules and coupling of electromagnetic responses (plasmons) within the array. In Figure 1, these steps are schematically explained. Each individual metamolecule is excited by the incoming electromagnetic wave (Figure 1b) and characteristic plasmonic resonances of the structure (metamolecule) will be present. Metamolecules can support a quasi-static electrical resonance [20],

$$\omega_r = \frac{1}{LC}. \tag{7}$$

In this case, the resonant frequency (ω_r) can be controlled through the inductance (L) and capacitance (C) of each individual metamolecule. However, when characteristic sizes of the structure correspond to a half-integer multiple of the effective wavelength, a geometrical resonance can also be excited,

$$\lambda_{r,N} = \frac{2\sqrt{\epsilon^*}l}{(2N+1)}, \tag{8}$$

where ϵ^* is the resonator's effective permittivity and N a positive integer. In such structures, the characteristic length of an individual metamolecule (l), controls the free space wavelength of the resonance ($\lambda_{r,N}$). The characteristic wavelength of a metamolecule can be considered as the effective length of the conductor that makes the unit cell. In several nanostructures this is considerably different from the unit cell itself, for example, if we consider the symmetric positive structure of the one represented in Figure 1a, the characteristic length (l) would be the length of the C-shaped "'wire"' and the horizontal bar below it. These resonances control the way electromagnetic energy is distributed within and scattered by the planar photonic metamaterial. When electromagnetic radiation interacts with plasmonic sub-wavelength structured metamolecules, electrons in the conduction band of the constituent material will start oscillating creating plasmons. A plasmon is a quasi-particle resulting from the quantization of plasma oscillations. These oscillations will occur inside the solid by transfer of linear momentum and energy from the electromagnetic wave to the solids' free electrons. Due to the electromagnetic interaction between metamolecules, a coupled electromagnetic response is produced (Figure 1c) resulting in the characteristic electromagnetic response of the planar photonic metamaterial array. The interaction energy from coupling two dipoles together, either electric or magnetic ones, can be derived considering a simple quasi-static picture [21]. For instance, let us consider a first approximation where only the dipole-dipole interaction is considered, although higher-order multipoles can play a substantial role in photonic metamaterials [22, 23]. If two dipoles with dipole moments p_1 and p_2 (either electric or magnetic) interact at center-to-center distance r, the quasi-static interaction energy Q_{int} is given by [24],

$$Q_{int} = \iota \frac{p_1 \cdot p_2}{4\pi\epsilon_0 r^3}, \tag{9}$$

where r is the distance between p_1 and p_2 and ι is the interaction index, which is +1 when considering purely transverse coupling or -2 for longitudinal coupling of the two dipoles with magnitudes p_1 and p_2. From equation 9 the interaction energy of the coupled metamolecules (dipoles) strongly depends on the distance (r) between them. This indicates that by displacing metamolecules relative to each other, the coupling energy can be tuned and the overall optical properties of the photonic metamaterial changed.

Now, if the plasmon oscillations are coherent and at an interface between two materials (at which the dielectric function changes sign), surface plasmons can be created and will propagate along the interface. The coherent oscillation of plasmons travels through the medium and can either be radiated into free space by coupling to a photon or be absorbed, depending on the the symmetry of the plasmonic mode. Coupling of photonic metamaterial plasmons to propagating photons results in the scattered field (intensity, polarization or phase). The coherent plasmonic scattered field will interfere with the incident electromagnetic wave of the photonic metamaterial. This new output electromagnetic response results from the overall electric and magnetic field interaction between the input electromagnetic wave and the electromagnetic characteristic response of the array, see Figure 1d. In this way, waves transmitted and reflected by a photonic metamaterial are formed. In summary, after traveling through a photonic metamaterial, the initial electromagnetic wave will be changed by the scattered electromagnetic field produced by the metamaterial. This scattered field results from the coupled plasmonic response of the metamolecules.

Electromagnetic coupling within the nanostructure and its dependence on dipole displacement implies that the optical properties of a planar metama-

terial can be controlled by changing the distance between rows/columns of metamolecules or even individual metamolecules themselves. Based on previous considerations, dynamic control over metamaterials optical properties is envisioned by displacing groups of unit cells within a nanomechanical planar photonic metamaterial. By doing so, coupling between the electromagnetic response of the different groups of unit cells will be changed and the resultant optical properties of the nanomechanical photonic metamaterial will be modified. An important factor to achieve high performance nanomechanical planar photonic metamaterial relies on the understanding and optimization of the design to be used. The electromagnetic response of three different designs was simulated for illustration purposes. Starting from the concept of nanomechanical planar photonic metamaterials built from bilayer structured nano-thickness membranes, geometric models can be studied using available Electromagnetic (EM) solvers, such as COMSOL Multiphysics.

The 3 different designs were chosen based on the existence of sharp edges known to result in strong field concentration and enhancement, and suitability of fabrication and actuation. All structures use the proven gold-on-silicon-nitride bridge actuator design concept used in earlier reconfigurable photonic metamaterials [25]. In fact, all designs are the result of a simple cut through both layers of a gold-coated silicon nitride membrane resulting in 3 different shapes of the gap between elastic bridges: meander cut, inverse triangle cut and chevron cut. In all cases, the considered model consists of a unit cell

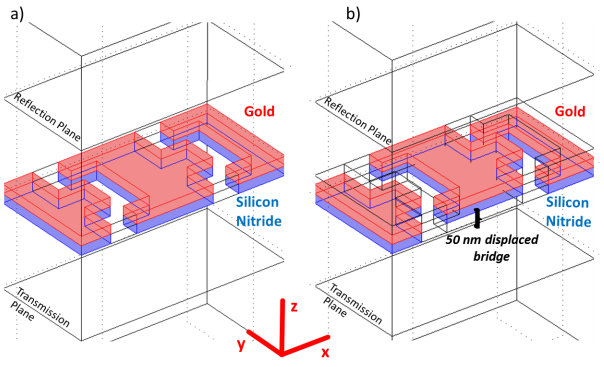

Figure 2. Nanomechanical photonic metamaterial design model. Models used for simulating optical properties of nanomechanical photonic metamaterial without (a) and with (b) displacement of the central bridge. The unit cell size is 1.2 μm $\times$ 600 nm, silicon nitride (blue layer) and gold (red layer) thicknesses are 50 nm for each and the central bridge displacement is 50 nm, for all 3 designs (meander cut shown). Wavelength dependent transmission is simulated using the electromagnetic waves module of Comsol Multiphysics.

size of 1.2 μm by 600 nm, composed of 2 bridges in such a way that displacement can also be simulated with minor changes, see Figure 2. Overall thickness of our metamolecules is 100 nm (50 nm SiN_x and 50 nm Au), periodic boundary conditions are used to simulate the optical properties of a metamaterial array and each material is simulated based on its wavelength dependent complex refractive index [26]. The electromagnetic input wave is polarized (E_x) perpendicular to the bridge orientation and its electric field amplitude is 1 V/m. Moreover, by simply changing the material properties assigned to different domains of the geometry, the optical properties of the displaced structure can be simulated (Figure 2 b) and compared to the stationary case (Figure 2 a). Different positioning of the bridges is achieved by attributing, for example, silicon nitride and gold material parameters to the bottom two layers in Figure 2 a, while maintaining the top layer defined as air. For the displaced strucutre (Figure 2 b), the bottom layer is defined as air while the top two layers are defined as silicon nitride and gold. The change of material properties for the different layers in our model corresponds to simulate a displacement of the central bridge relative to the outside ones by 50 nm (thickness of one layer) in the out of the metamaterial plane, z direction.

By integrating the overall power outflow over the transmission plane for each wavelength and normalizing it to the incident wave's power, one can plot the transmission spectra for each studied design, with and without displacement. Bigger differences in transmission (or reflection) of the nanostructure between these two cases will, in principle, lead to increased tuneability of our nanomechanical photonic metamaterial for the same external stimulus. The wavelength-dependent transmission (600-1800 nm wavelength) for all three designs with and without displacement was calculated considering light polarized perpendicular to the orientation of the bridges, see Figure 3. As can be seen from the spectra, similar properties - comparing the displaced and non-displaced cases for each design - are obtained for wavelengths smaller than the unit cell dimension (1.2 μm) in the light polarization direction. It should be mentioned that model's accuracy when dealing with diffraction of light (below 1.2 μm) was not characterized, however for longer wavelengths where diffraction is nonexistent the model as shown to work well. Therefore, below 1.2 μm we can only conclude that despite displacement of the beams, no clear transmission changes were observed while a possible change in the diffraction pattern is observed. At 1.2 μm all structures show an extra bump for the displaced trace which sits exactly where the wavelength reaches the unit cell size. Moreover, each of the de-

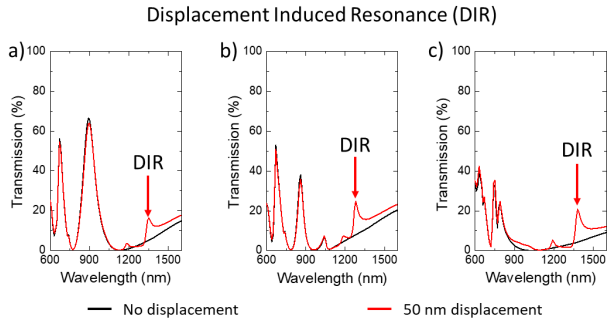

Figure 3. Calculated transmission spectra for different nanomechanical photonic metamaterial designs. a) Meander cut design, b) inverse triangle cut and c) chevron cut. Simulation results are obtained with (red line) and without (black line) displacement for the 3 different designs. In all cases, incident light is x-polarized (1V/m) and bridges consist of layers of 50 nm SiN_x and 50 nm Au. Dashed lines show the wavelength at which a new resonance appears upon a 50 nm out-of-plane displacement of every second bridge.

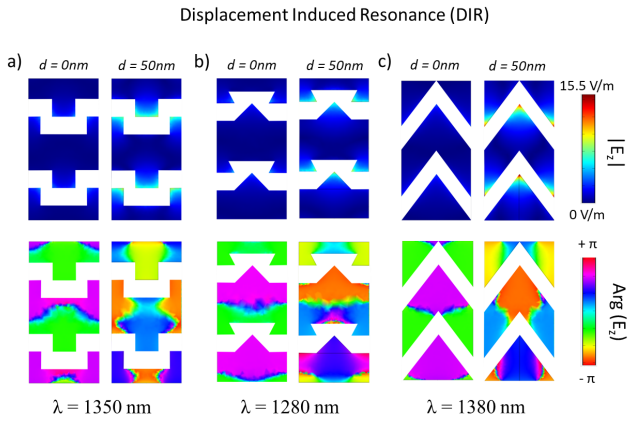

Figure 4. Calculated near-field maps for different photonic metamaterial designs. a) Meander cut at 1.35 μm wavelength, b) inverse triangle cut at 1.28 μm and c) chevron cut at 1.38 μm. In all cases the results plotted are abs(E_z) in the top row and arg(E_z) on the bottom one, 10 nm above the gold surface of each bridge.

signs presents an extra small resonance at wavelengths longer than the structure's period of 1.2 μm when the structure is only 50 nm displaced. From Figure 3 we can obtain the wavelengths where these resonances appear, these being 1.35 μm for the meander cut, 1.28 μm for the inverse triangle cut and 1.38 μm for the chevron cut. At these displacement induced resonances (DIR) wavelength our designs are effectively metamaterials behaving as effective homogeneous media, since the wavelength of interaction is bigger than the metamaterials' unit cell.

It is interesting to study the resonances that appear as a result of displacement in the metamaterial regime. Amplitude and phase maps of the electric near-field along the propagation direction (E_z) are extracted, 10 nm above the gold surface on every bridge, see Figure 4. Such maps indicate the oscillating charge distribution of the plasmonic mode excited by the incident wave. The magnitude of the electric near-field, abs(E_z), is shown in the top row of Figure 4. All results are plotted on the same scale and were obtained for the characteristic resonant wavelength of each structure. Looking into the phase maps, bottom row of Figure 4, without displacement, charges on neighboring bridges oscillate in phase. Results are considerably altered upon displacement of every second bridge. For all designs, displacement results in resonant and approximately anti-symmetric charge oscillations on neighboring bridges. This indicates a breaking in the symmetry of the structure and corresponds to the excitation of a resonant "trapped-mode" [27]. Without displacement, all 3 designs are non-resonant and therefore their excitation is weak.

However, when every second bridge is moved 50 nm towards the light source, resonant behavior at each designs' DIR wavelength is clear. Electric filed enhancement is clearly concentrated at the edges of the structure and is several times higher for the chevron design when compared to meander and inverse triangle designs. Amongst the 3 studied designs the strongest enhancement of the electric field is observed for the chevron cut with an increase in the magnitude of E_z of about 15 times.

Through an extensive and careful study of other possible designs, displacement directions (stretching or movement in plane) and introducing new materials, there is still a lot of room for optimization of responses and maximization of changes. Many other designs for dynamic control over phase, intensity and polarization of light can be envisioned. Here we gave a basic introduction to the origin of tuneable properties of nanomechanical photonic metamaterials and how such metamaterial designs can be optimized through simulation in order to enable the reader to explore their own ideas.

2. Actuation mechanisms

Dynamic spatial reconfiguration of a metamaterial structure requires an actuation mechanism and several approaches to actuation will be discussed in this section. Reconfigurable photonic metamaterials based on Micro-Electro-Mechanical Systems (MEMS) have been realized for THz and sub-THz frequencies [28–33] and recently shrunk to the optical spectral range [25, 34, 35]. Tuning of the optical properties of these materials results from structural reconfiguration of

the photonic metamaterial. Sub-wavelength scale structuring of a noble metal film supported by a dielectric membrane of nanoscale thickness can be used to make mechanically reconfigurable metamaterials suitable for the optical spectral range. Ou *et al.* demonstrated tuneability using 3 different mechanisms of actuation based on this nanomembrane approach [25,34,36]. Interaction of an electromagnetic wave with a densely populated metamaterial, where metamolecules are strongly coupled (equation 9), will alter the wave by plasmonic phenomena. While previous simulation results provide us with useful insights regarding near-field interactions of neighboring bridges for the different designs, also mechanical considerations about the design should be taken into account. For a full review on reconfigurable nanomechanical photonic metamaterials and the latest advances on the field see Ref [37].

In principle, the stronger the coupling, the easier it should be to observe displacement-induced transmission changes of our photonic metamaterial. However, if the design is too stiff, available forces for tuning might not be strong enough to achieve significant bridge displacement against the structure's elastic forces. Since we aim to tune the optical properties of metamaterial structures by reconfiguring their nanoscale components in response to different control signals, estimates on the magnitude of available forces should be made. Therefore, not only electromagnetic properties of structures but also mechanical ones are important to achieve significant tuning of optical properties.

In this section we will discuss the mechanical properties of bi-layer designs, as well as, estimate the available forces using different actuation mechanisms. In the end, by changing the physical arrangement of the nanoscale metamolecules we change their coupling (equation 9) and therefore the optical properties of the photonic metamaterial array. Large modulation of optical properties will be provided by a design with strongly interacting bridges that have a weak elastic restoring force. It should be pointed out that all estimates and considerations presented on the following subsections are made considering the central part of the nanostructures (beams), since it is the spatial region where the displacement is bigger and from where the optical properties are measured. Several actuation mechanisms can be considered to reconfigure nanomechanical photonic metamaterials either with an electrically conductive path present or not. Considering designs where we have an electrically conductive gold layer covering the dielectric bridges, electric signals can be used to produce displacement. Regardless of presence of such a path, thermal or optical actuation can be considered.

Here we will discuss and estimate several actuation mechanisms: thermal, electrothermal, electric, magnetic and optical actuation. Later, considerations will be made on the different actuation mechanisms based on their simplicity and on the achievable displacements.

2.1. Restoring forces

In order to achieve tuneability in the visible part of the electromagnetic spectrum, structurally reconfigurable photonic metamaterials propose to manipulate light by changing the relative arrangement of their plasmonic building blocks, i.e. thousands of metamolecules. Moreover, by being fabricated from bi-material layers, i.e. metal on top of dielectric, planar metamaterials which are reconfigurable by ambient temperature changes or electrostatic actuation have been realized. Bi-material layered structures can be actuated by temperature changes based on different thermal expansion coefficients to engage displacement and different layers can provide both a mechanical support (dielectric) and a plasmonic material (metal). Elements of nanomechanical photonic metamaterials can often be represented as nanobeams. At the nanoscale, electromagnetic forces and thermally actuated displacements act on such nanobeams and are comparable with elastic forces of the supporting structure. In general, the elastic restoring force of such a nanobeam with circular cross-section and supported on both ends can be described as [37],

$$F_{Elastic} = 6\pi E \frac{D^4}{L^3} x, \tag{10}$$

where, E is the Young's modulus, L is the length, D the diameter and x the displacement of the nanobeam. These parameters are shown in Figure 5, considering a general design. Using equation 10, we can estimate the force needed to achieve displacement. Gravity can be neglected for the beam structures of picogram-scale weight that have typical beam lengths of tens of microns.

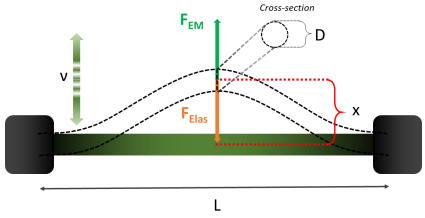

Figure 5. Elastic force at the nanoscale. A nanobeam anchored at both ends of length L, diameter D and Young's modulus E. Using different external stimuli it is possible to drive the nanobeam (with characteristic frequency, ν) against its elastic restoring force.

In order to estimate and understand the mechanical response of such systems, restoring elastic forces and available actuation forces need to be estimated. As for the restoring elastic force, we can now estimate its magnitude for the designs discussed in the previous section, i.e. meander cut, triangle cut and chevron cut. All designs can be simplified as beams with circular cross section with diameter of 100 nm. The simulated structures will correspond to 3 such beams next to each other (i.e. 3x bigger force), since the cross section is not circular and we want to account for the beam width (aprox. 300 nm). Amongst the simulated designs and for restoring force estimates purposes, the meander cut and inverse triangle may be approximated by straight silicon nitride beams, despite the structured sides. The spring-like design of the chevron structure can be approximated also by a straight beam but with much longer effective length, accounting for the zig/zag elastic design. For a typical beam manufactured from a low stress (S $\leq$ 250 MPa) silicon nitride membrane, we can expect a restoring force on the order of 3.9 nN (1.3 nN per 100nm circular beam, 30 μm long) for a displacement of 100 nm. Considering Young's modulus of silicon nitride, E_{SiN_x} = 297 GPa used as substrate and the additional gold layer (E_{Au} = 79 GPa), the effective Young's modulus based on 50% SiN_x and 50% gold is E_{Eff} = 188 GPa. Therefore, for the more elastic chevron design the restoring force will be weaker for the same displacement, since it is a longer beam (effective length). Following equation 10, increasing the length of the beam (L^3) or decreasing its diameter (D^4) are the most effective ways to lower the restoring elastic force, since small changes have exponential influence. Clearly, careful design of the beams supporting or self-containing the metamolecules can dramatically modify its elastic response. Moreover, choosing materials with lower Young's modulus (or lower stress), using more elastic designs (meandering of bridges) or tapering the ends of the beams, can also result in reduced restoring elastic force, leading to bigger displacements for the same actuation forces. Nevertheless, the above considerations indicate that forces on the nano-Newton scale will be required to achieve significant deformation of nanomechanical photonic metamaterials based on silicon nitride bridge beams.

The next section will provide estimates on the magnitude of the available forces for reconfiguring such nanostructures.

2.2. Thermal Actuation

Thermally reconfigurable photonic metamaterial structures are based on materials having different thermal expansion coefficients. Combining such concept with nanomembrane technology, which provides very thin, flexible dielectric substrates, temperature changes can lead to displacement of bi-layer nanobeams. Evaporation of a plasmonic metal on one or both sides of such substrates allows the fabrication of an array of plasmonic metamolecules supported by pairs of nanobeams cut from the membrane and designed in a way that one string of the pair exhibits temperature-activated deformation while the other does not. These bridges can be spatially repositioned by changing the ambient temperature or engaging Joule heating in the conductive layer. In the first case, half of the nanobeams are gold-covered on both sides, while the other half are only covered by gold on one side. By changing ambient temperature, one can engage displacement of one bridge (metal-dielectric) relative to the other (metal-dielectric-metal) and this results in optical changes. When the temperature of the metamaterial changes, only the asymmetrically layered bridges that are gold-covered on only one side will bend due to different thermal expansion coefficients of gold and silicon nitride.

In the second case, currents can be applied to the metallic layer of a metamaterial and flow (by design) along every second bridge in order to change the electromagnetic interaction between neighbouring bridges. Joule Heating of the current-carrying, bilayered bridges can result in out of plane movement of hundreds of metamolecules. For both cases, the bridges with no thermal load will remain static since either structural symmetry or lack of Joule heating will not allow displacement.

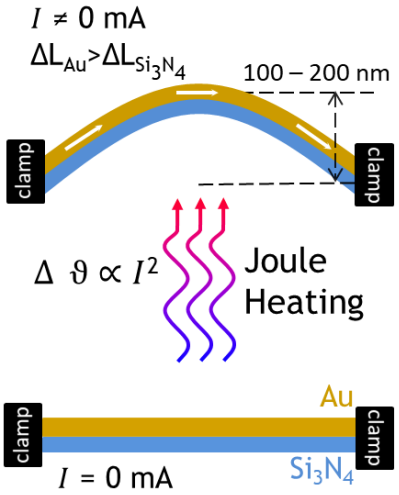

Figure 6. Electrothermal actuation concept. Upon electric current (I) application, a bilayer beam fixed at both ends will experience Joule heating which will result in out of plane bending of the beam ($\Delta L_{Au} > \Delta L_{Si_3N_4}$). Such bending can result in hundreds of nanometres displacement at the centre of a beam that is 10s of microns in length. Also, environmental temperature changes could produce the same effect in the nanobeams at much slower timescales.

Heating will increase the average distance between ions due to their vibrational energy increase and will result in a volumetric expansion of the material. Materials that expand at the same rate in every direction are called isotropic, for these materials the area and linear thermal expansion coefficients may be calculated from the volumetric coefficient. Depending on the application or dimensions considered important, different coefficients may be considered. In our case, the linear expansion coefficient is considered due to the 1D nature of our structures were the length of the bridges is much bigger than width and thickness. For this situation, the variation (ΔL) of the bridges length (L) for a certain temperature change ($\Delta\vartheta$) is related by the linear expansion coefficient (α_L):

$$\frac{\triangle L}{L} = \alpha_L \Delta\vartheta. \tag{11}$$

Thermal expansion coefficients vary from material to material and if we consider a bilayer structure of two different materials, one dielectric (e.g. silicon nitride, $\alpha_L = 2.8 \times 10^{-6}/K$) and one metal (e.g. gold, $\alpha_L = 14.4 \times 10^{-6}/K$), the different change in lengths results in bending of the structure. For example, following equation 5 of reference [38], a displacement of approximately 3 nm per degree Kelvin can be expected for a silicon nitride and gold bilayer beam with thickness ratio of 1. The changing distance between metamolecules or between arrays of metamolecules (nanobeams) modifies the plasmonic coupling (equation9) and the electromagnetic response. Figure 6 illustrates how thermal actuation can be driven by Joule heating where out of plane displacement of a bilayer beam results from differences in thermal expansion coefficients. Hundreds of nanometres out of plane displacement are achieved and the influence on optical properties has been reported to be around 50% of relative transmission changes [25, 35]. Following previous reference [38], a work per volume for thermal actuators can be estimate and translated to a thermal force ($F_{Thermal}$) of about 1 nN per nanometer displaced. Therefore, per Kelvin degree raise in temperature, 3 nN of thermal force will act at the center of the bilayer nanobeam. Thermal actuation can provide large contrast in the optical properties of the planar photonic metamaterials by achieving big displacements.

Despite achieving a fully reversible mechanism to tune metamaterial optical properties, this work has the drawback of being relatively slow: the reaction time (characteristic heating/cooling time), τ, depends on the thermal conductivity of materials involved and the geometry of the string. The reaction time (s) as function of thermal conductivity, κ (W/m.K), and string length, L (m), is given by:

$$\tau \approx \frac{L^2 C_L}{12 A \kappa}, \tag{12}$$

where, C_L ($J/K.m$) is the heat capacity per unit length and A (m^2) the cross-section of the string. Therefore, depending on the capacity of the material to receive heat to achieve certain temperature, its thermal conductivity, the length and the shape of the beams, thermal equilibrium will be achieved at different rates. For metamaterials with an overall size of tens of micrometers, the response time is typically on the microsecond to millisecond scale. Such response times are still useful in a wide range of applications where process are relatively slow such as, chemical sensing or monitoring biological processes. Moreover, the response time of thermal actuation can be reduced by displacing smaller components of the unit cell (instead of several unit cells in a nanobeam), which will lead to faster thermally actuated metadevices with wider range of applications. Alternatively, there are other mechanisms which can provide almost unlimited fast responses and be useful for telecommunications and optical computing.

2.3. Magnetic Actuation

While thermal actuation promises large tuning, it is inherently slow as it is limited by the cooling timescale on the order of microseconds. In order to overcome this disadvantage, one promising approach is to use the Lorentz force on a current carrying wire placed in a magnetic field to reconfigure nanomechanical photonic metamaterials. This allows the metamaterial's optical properties to be conveniently modulated by the applied current and thus it has the potential of being a practical method for fast control of metamaterial properties [35], as well as, providing a large reciprocal magneto-electro-optical effect [39]. The practical realization requires currents to be applied to selected reconfigurable parts of the nanostructure, which needs to be placed in a magnetic field oriented perpendicular to the current flow. Due to electric current application and the bilayer nature of the nanobeams, Joule heating will create a uniform thermal background [39]. This means that the magnetic actuation will act on top of pre-displaced nanobeams resulting from the thermal force actuation. The direction of the resulting magnetic force can be reversed by reversal of the direction of either current flow or magnetic field. In Figure 7 the concept of Lorentz force tuning of a nanomechanical photonic metamaterial bridge is illustrated.

Assuming realistic values we can estimate the Lorentz force exerted on metamaterial bridge actuators. Considering the bridges as current carrying wires,

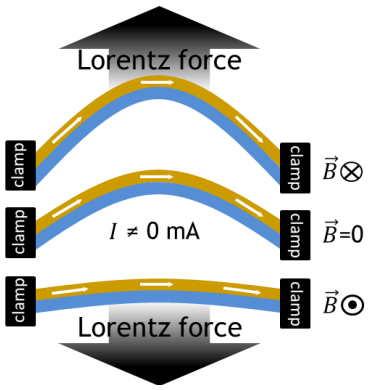

Figure 7. Magnetic actuation concept. Moving charges (electrical currents) in the presence of a magnetic field oriented perpendicular to the current experience the Lorentz force. Such force can be used for fast reconfiguration of metamaterials with beam displacement in a chosen direction.

the force acting on a current in a magnetic field is given by,

$$\vec{F} = L\vec{I} \times \vec{B}. \tag{13}$$

Considering a current of 1 mA and a magnetic field of 0.1 T, forces of about 100 pN per 1 μm of nanowire length are achieved. On a thermal background, such magnitude of magnetic force only results in a few tens of nanometres of displacement. Nevertheless, around 25% relative transmission changes have been reported using purely magnetic actuation [35, 39], due to the strong coupling between metamolecules separated by nanoscale gaps. In these works, authors do not report on hysteresis and drive the structures up to 200 kHz, showing fast light modulation for purely magnetic actuation.

Comparing to thermal actuation, magnetic one can provide extremely fast response times since there is no need to dissipate the heat. The thermal background present (in equilibrium) will allow for fast magnetic tuning, when changing the magnetic field intensity and/or direction. In this case, since there is no need to cool down the nanobeams, actuation frequency only depends on the design of the nanobeams (or unit cell) and electric circuit used for actuation. Stronger magnetic fields and higher currents can be used and displacements further increased. As before, addressing individual unit cells of a metamaterial will allow for faster metadevices and spatial resolution. Finally, the Lorentz force can significantly deform nanomechanical photonic metamaterials and thus be used to control their optical properties.

2.4. Electric Actuation

When an electrical path is present in the nanomechanical photonic metamaterial design, another possible way to engage displacement is by exploiting electric forces to reposition the nanobeams. Such electric signals can provide different forces to achieve displacement and therefore changes in the optical properties of the metamaterial. Actually, two kinds of electric forces can be used to address nanomechanical photonic metamaterials. Firstly, lets think of the Ampère force that depends on the current (I) in the nanobeams and the distance (d) between them. Joule heating will also be present in this system, however it will be homogeneous along the entire metamaterial and act perpendicularly to its plane, pre-displacing the nanobeams. The Ampère force will act on the metamaterial plane and it may be understood as the repulsion force acting between a current carrying wire and the magnetic field caused by the current in the neighbouring one.

$$F_{Amp} = \frac{\mu_0 I^2}{2\pi d} L. \tag{14}$$

Here, μ_0 is the vacuum permeability. The achievable Ampère force (F_{Amp}) tends to be small when compared to previous approaches. For I = 1 mA and d = 500 nm, the Ampère force is about 0.4 pN per 1 μm of nanowire length L. Another possible use for the electrical path present in the sample would be to engage Coulomb forces (F_{Coul}) that depend on the potential difference V between the nanobeams of our designs, their diameter and the distance between them. Ou et *al.* [34] developed a type of metamaterial operating in the optical part of the spectrum, in which the nanostructure is actuated by the F_{Coul}. Such force acting on typical reconfigurable photonic nanostructures can be approximated by,

$$F_{Coul} = \vartheta(D,d)\frac{\pi\epsilon_0 U^2 D}{2d(d-D)} L, \tag{15}$$

where, $\vartheta(D,d)$ is a dimensionless parameter that takes a value close to 1 for realistic geometries, D the diameter of the nanowires, d the distance between them, ϵ_0 the permittivity of vacuum and U the applied voltage. Similarly to previous actuation mechanisms with electrical signals, marginal heating of the nanostructure might occur. As before, the movement caused by this marginal thermal actuation will be perpendicular to the direction of tuning induced displacement and therefore can be neglected. For U = 1 V, D = 100 nm and d = 500 nm, the Coulomb force is about 5 pN per 1 μm of nanowire length L. The charged plasmonic metamolecules which are supported by pairs of parallel strings cut from a nanoscale thickness flexible silicon nitride membrane move due to electrostatic

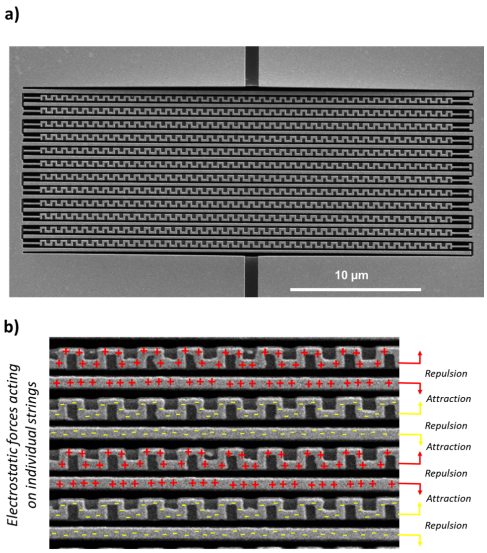

Figure 8. Electrostatically nanomechanical photonic metamaterial. [34] a) Scanning electron microscope image of the device, black colour is the gap, light grey is gold and dark grey is the supporting silicon nitride membrane. b) Close up of a section of the metamaterial pattern. An applied voltage results in an acting electrostatic force that moves the bridges in plane. Negative charged bridges (yellow) will repel each other and be attracted to the positive charged (red) bridges or *vice-versa*.

attraction and repulsion, and thus repositioning of metamolecules is achieved, see Figure 8. These strings of picogram mass and only 100 nm thickness can be synchronously driven to megahertz frequencies to electromechanically reconfigure the metamolecules and dramatically change the metamaterial's transmission and reflection spectra, thus giving rise to a colossal electrooptical effect. Using Coulomb forces and in-plane movement of the nanobeams, authors were able to engage two different modes of operation: (i) analogue tuning, where over a range of voltages the structure's optical properties can be changed continuously (up to 8% optical signal modulation); (ii) a step-like "digital" change of the optical properties (switching with 250% contrast), where the electrostatic force overcomes the elastic restoring force. For case (i), the magnitude of the optical changes is quite small comparing to purely thermal or magnetic actuation, despite the strong coupling and considering equation 9. This can be explained by the in-plane nature of the tuning which, despite changing drastically the distance between dipoles, does not allow for large displacements without permanent switching. Such switching brings us to case (ii), where huge changes in the optical properties are achieved at the cost of non-reversibility. When the nanobeams are brought closer and closer together, they will eventually touch and get stuck together. This switching will lead to great optical contrast but the metadevice will be permanently "'switched"', losing the ability to change its optical properties.

Another versatile solution is based on actuated Salisbury screen designs [40–42], where the electrostatic force between a metasurface or metasurface strips and a ground plane controls the optical properties of the device. Such structures have been shown to act as electro-optical modulators and could provide dynamic control over essentially any optical functionality metasurfaces can provide [43, 44].

2.5. Optical Actuation

Finally, one of the most ambitious and interesting ways of reconfiguring photonic metamaterials is using light itself. Light by light nanomechanical photonic metamaterials have already been demonstrated [36], see Figure 9. By exploring optically induced forces that act on a plasmonic metamaterial array, authors

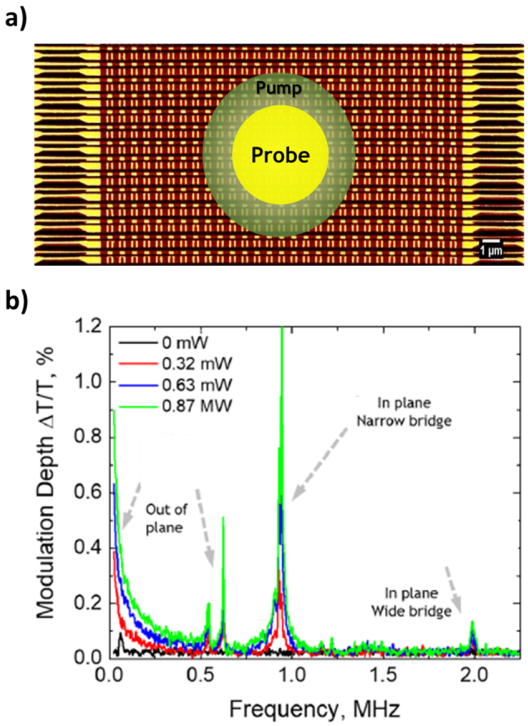

Figure 9. Optically nanomechanical photonic metamaterial. [36] Nanomechanical photonic metamaterial where tunability of optical properties is driven by optical forces, a) a pump beam modulating a probe beam at a different wavelength and achieving the result shown below. b) Transmission modulation at the probe wavelength as a function of pump modulation frequency for different pump powers. Each modulation depth peak has a characteristic mechanical mode identified by the arrows. Adapted from [36]

engaged nanoscale reversible displacements of its small and light building blocks. Light induced oscillating dipoles are engaged in order to produce a time-averaged optical force that is proportional to the incident light intensity, I_{light} and the illuminated bridge length L,

$$F_{Optical} \propto I_{light} L. \tag{16}$$

When such gold plasmonic nanowires of diameter D = 100 nm, length L = 500 nm and spacing d = 300 nm are illuminated by light with wavelength λ = 925 nm and intensity P = 1 mW μm^2, the repelling optical force between them is about 1.5 pN. Using nanomembrane technology and plasmonic structures, optically-induced forces drive the nanostructure at up to MHz modulation rates. By using a pump beam (shown red), the authors modulated another, weaker probe beam of light (shown green) at a different wavelength. Recently, it has been shown in an all-dielectric nanomembrane metamaterial that optical forces can drive actuators on the size-scale of an individual meta-molecule (about 1 μm) at frequencies of more than 100 MHz [45]

At first sight, almost all available forces have been engaged and explored to achieve reversible, high contrast and high frequency tuning of optical properties. The forces used and their understanding is not too complex and can be easily adapted to other designs and systems. The challenges to achieve metadevices are now focused on the nanofabrication of such nanostructures and their optimization.

Next, this tutorial will focus on nanofabrication solutions and challenges for nanomechanical photonic metamaterials.

3. Fabrication of Nanomechanical Planar Photonic Metamaterials

A lot of the progress in photonic metamaterials research only became possible due to developments in nanofabrication technology achieved over the last two decades. However, in order to keep pushing the boundary further, more improvements and merging of technologies for fabrication of structures with nanometre resolution is imperative. If one can fully control nanometre scale fabrication and even achieve sub-nanometre resolution, high quality photonic metamaterial can be realized and further lower their wavelength of operation. Moreover, sample fabrication and processing becomes increasingly important when concepts must be put forward into devices. If fabrication does not reach a minimum level of quality, performance will be degraded or could even vanish completely. The requirements of photonic metamaterial samples, depending on the final applications, are becoming increasingly more complex with high levels of accuracy and precision needed. Nanofabrication of optical metamaterials is extremely challenging and requires the creation of features at deep subwavelength scale. The required feature sizes are smaller than the resolution of conventional photolithography and therefore advanced technologies are being employed. Nanoimprint, interference optical lithography, direct laser writing, electron beam lithography (EBL) and focused ion beam (FIB) milling are just some examples [46, 47]. Some of these technologies achieve cost efficient, high-volume fabrication of micro- and nanoelectronic devices, but require masks/stamps, chemical solutions or highly energetic (thermal) processes which can be a disadvantage for prototyping.

Also, to achieve high resolution nanostructures, substrates need to possess a minimum mechanical and thermal stability for processing. Usually, processes are highly energetic and consequently plasmonic thin films should attain minimal mechanical resistance and provide good enough thermal energy dissipation. Several techniques can be used in order to obtain metallic plasmonic thin films. For nanomechanical photonic metamaterials, the goal is to achieve metallic thin films with plasmonic properties, usually made out of gold, with no strict requirements in terms of electrical properties or morphology. The crucial parameter to take into account is the film thickness. While thin film quality is important for metamaterials, the metal film thickness is crucial as plasmonic properties depend on the photon penetration skin depth of the metal. The skin depth can be calculated as [48],

$$\delta_s = \frac{1}{\frac{\alpha}{2}}, \tag{17}$$

where $\frac{\alpha}{2}$ is the attenuation constant and is identical to the (negative) real part of the propagation constant, the ratio of the amplitude at the source of the wave to the amplitude at some distance x. For a typical plasmonic metal such as gold, the skin depth ranges between 6.2 nm for 2 μm wavelength and 2.8 nm for 400 nm wavelength, meaning that a 10 nm thick gold film should be enough to attain good plasmonic responses. These values are characteristic of each material and should always be considered in the photonic metamaterial design. Now, if we want to structure such a extremely thin film with FIB we might encounter some limitations. For example, structuring a 20 nm gold film supported by a 50 nm silicon nitride membrane might result in over milling of the metallic layer in order to completely cut through the dielectric. This means that the design intended to be patterned will not be possible to reproduce due to the physical limitations of the system. In order to achieve nanomembrane-based high quality nanomechanical photonic metamaterials, a minimum gold thickness of

30 nm has been used. However, when fabricating free-standing plasmonic metamaterials consisting of a very thin metallic/plasmonic layer, a minimal thickness of about 50 nm is needed to achieve same quality nanostructures, considering the absence of the mechanical and thermal support given by the silicon nitride membrane. Thinner free-standing plasmonic layers will deform upon FIB interaction, due to ion impact and thermal load, making structuring problematic. The limitations here presented are a mere example, since each system will possess its own limits depending on material properties and optimization of the nanofabrication conditions.

A lot of work has been done recently concerning fabrication at the nanoscale, exploring new techniques, increasing resolution levels and reproducibility. Hopefully this piece of work reflects on such advances and brings solutions and ideas to the metadevices realm.

3.1. Focused Ion Beam

Demand for miniaturization in electronics and optoelectronics increased the number and accuracy of fabrication techniques able to deliver sub-micron features. Several lithographic methods [49, 50], including electron beam lithography [51], were developed in recent years to achieve resolutions below 100 nm. Another technique that recently emerged is nanoimprint [52] which uses a stamp in order to reproducibly pattern a surface. However, both technologies have disadvantages. Considering, for example, any type of photolithography, the need for a photomask is inefficient and restrictive while high-resolution masks have prices well above £10k, making this technique too expensive for prototype fabrication and development. Lithography with multi-step techniques involving chemical procedures that require optimization can damage nanoscale structures, for example due to surface tension in liquids. Nanoimprint promises large area patterning and cheap mass-production of identical copies of the same photonic metamaterial, however, the cost of stamp fabrication makes it unsuitable for obtaining research samples, where almost every sample needs to be different.

Focused ion beam as proved to be a powerful tool regarding nanofabrication for prototyping. Despite expensive either in cost as in time, it is an extremely precise and elegant tool which as allowed us to manufacture the smallest features and engineered very interesting solutions. Considering low-volume fabrication of nanodevices like nanomechanical planar photonic metamaterials for prototype device development, focused ion beam milling, despite being time consuming, stands out as the best choice. This flexible technology allows the fabrication of a large range of structures in a single step process with spot size of 5 nm and line resolution of 30 nm without involving chemical precursors. The basic functions of the FIB require a highly focused beam. The smaller the effective source size, the more tightly can the ion current be focused to a point. Unlike the broad ion beams generated from plasma sources, high-resolution ion beams are defined by the use of a field ionization source with a small effective source size on the order of 5 nm. Of the existing ion source types, the liquid metal ion source (LMIS) provides the brightest and most highly focused beam. There are a number of different types of LMIS sources, the most widely used being a Gallium-based (Ga) blunt needle source. Ga has clear advantages over other LMIS metals such as In, Bi, Sn, and Au because of its combination of low melting temperature (30°C), low volatility and low vapour pressure. The low melting temperature makes the source easy to design and operate. Because Ga does not react with the material defining the needle - typically tungsten (W) - and evaporation is negligible, Ga-based LMISs are typically used in commercial FIB systems [54, 55]. Other ion sources can be used has the gas field ion sources (GFIS) using helium (He) or neon (Ne). Such ion sources have the advantages of achieving sub-nanometer resolution through minimization of the chromatic and spherical aberration of the imaging species (He or Ne). Disadvantages relate mainly with milling times, which are too long due to the small currents available with GFIS,

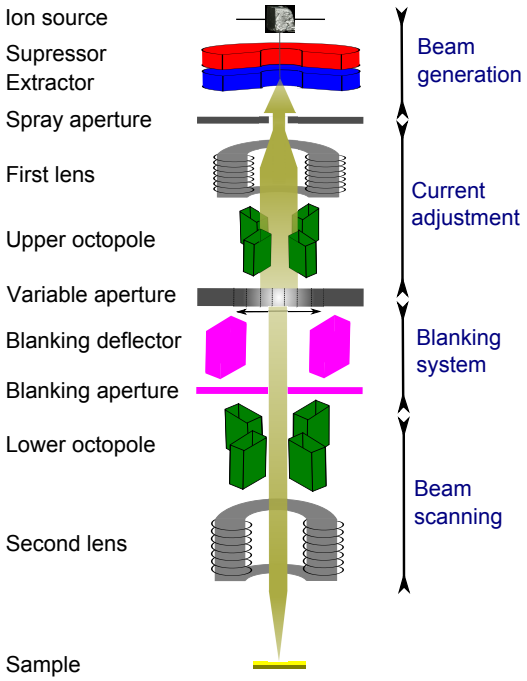

Figure 10. Schematic of the focused ion beam system composed of 4 subsections: beam generation, current focusing adjustment, beam blanking system and beam scanning. Adapted from [53]

and the large interaction volume, which will result in more damage of the subsurface material [56].

The most important components of such commercial system are: the ion column, the work chamber, the vacuum system, the gas injection system and the computer controlled user interface [53]. A typical diagram of a FIB column is shown in Figure 10. The structure of the column is similar to that of a scanning electron microscope (SEM) but instead of an electron beam it uses a gallium ion (Ga^+) beam. Typically, a vacuum of about 1×10^{-7} mbar is maintained inside the column to enable emission, focusing and manipulation of the ions. At the source, liquid Ga is extracted from a liquid source by electric field induction upon high voltage application. Ions of Ga will then be accelerated down the column and pass through a first aperture for first profile shaping. The ion beam energy is typically between 2 and 30 keV. Then, the ion beam is condensed by the first electrostatic lens while the upper octopole adjusts the beam stigmatism. Using the variable aperture mechanism, the beam current can be varied, usually between 1 pA and 22 nA. Depending on the beam current one can obtain either a fine beam for high-resolution imaging or a strong beam for fast and rough milling. Blanking of the beam is realized by the blanking deflector and aperture in order to promptly blank the beam during fabrication. The lower octopole is used for raster scanning the beam over the sample in a user-defined pattern, facilitating the most intricate and twisted designs with high resolution. Finally, the beam is focused to a fine spot with the second electrostatic lens, enabling a best resolution in the sub 5 nm range. In FIB technology, imaging and milling with Ga^+ ions will always result in Ga^+ ion implantation in the sample, see Figure 11 . In order to avoid ion implantation during sample imaging, most modern FIB instruments supplement the FIB column with an additional SEM column so that the instrument becomes a versatile "dual-beam" platform. The ion beam and electron beam are placed in fixed positions and share their focal points at the "coincidence point", an optimized position for the majority of operations, including FIB sample direct writing [55]. The SEM part can be used not only to search and image the sample area for FIB processing but also to monitor the process of FIB milling in real time.

Based on the ion-solid interactions, there are three main working principles of an FIB system, namely imaging, milling, and ion beam induced deposition [53]. Figure 11 shows these modes which are relevant for nanomechanical photonic metamaterials fabrication. Controlling, for example, emission energies (5-10 keV), FIB system can be used for high resolution imaging of samples (Figure 11a). Such process is destructive and should be carefully controlled to minimize alteration of sample properties. Due to the detection of low energy secondary electrons and/or secondary ions, FIB is especially sensitive to the surface topography and to the work function of the surface [57]. The FIB secondary electron signal will thus depend on the chemical nature of the surface as well as its morphology. Moreover, FIB provides a greater sensitivity of an incoming beam to the crystalline structure of the sample. In a crystalline sample it is possible for the primary ions to channel if the orientation of the crystal is aligned with the beam. In this case, the ions travel between the columns of atoms and their range can be quite large. Since a longer range implies fewer interactions (per unit length) between ion and sample, the number of secondary electrons produced will be lower if the crystalline sample is oriented in certain directions relative to the beam. This effect induces image contrast variations depending on small changes of the angular orientation of the sample, which is called 'channelling contrast'. Despite the ability to provide higher resolution imaging than the common SEM systems, we must keep in mind that contamination with the ion species used is unavoidable, Figure 11.

The most important operation mode of an FIB system, for nanomechanical photonic metamaterials fabrication, is the milling process. In such mode, higher energies for the ion beam are used (10-30 keV) to promote sputtering of sample's material and allow milling (Figure 11b). Ion milling is a method of material removal by means of physical sputtering phenomena. The sputtering process involves the transfer of momentum to surface and near-surface atoms from the incident ions through a series of collisions within the solid target. If the ion beam impinges on the target vertically there must be enough momentum reflected from the solid to eject one or more surface atoms. Therefore, the sputtering rate, which is defined as the ratio of the number of ejected atoms to the number of impinged ions, is a function of the angle of incidence of the ion beam as well as the mass and energy of the ions, the mass of the target atoms and the nature of the target atomic structure. FIB milling is carried out with repetitive scanning over a designated area. Arbitrary surface topographies can be created by controlling the scanning pattern, scanning location, and ion dosage. Typically, with a focused 30 keV Ga^+ ion beam of less than 5 nm diameter, structures with less than 30 nm features can be realized. The minimal milling linewidth is about 50 nm. Further in this tutorial, typical examples of nanomechanical photonic nanostructures fabricated using focused ion beam milling will be shown. The FIB milling process can be further enhanced by introducing a specific gas (such as XeF_2) into the work chamber.

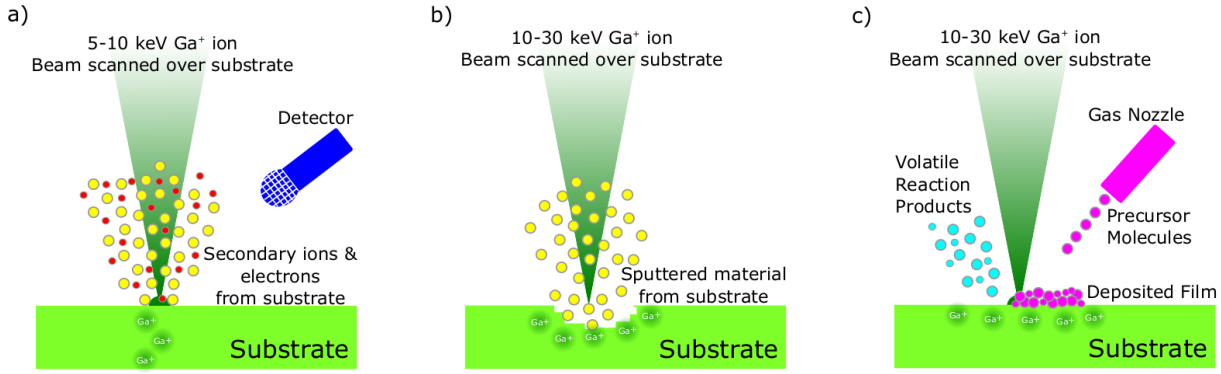

Figure 11. Focused ion beam operation modes. FIB systems can be operated in distinct modes including a) ion imaging b) ion beam milling and c) ion induced deposition. Adapted from [53]

It will increase the etching rate and the selectivity towards different materials by chemically facilitating the removal of reaction products. This technique is called gas-assisted etching [58].

Finally, the third operation mode is ion induced deposition of thin films (Figure 11c). By introducing a gas flux through a nozzle in the vicinity of the ion beam we can grow thin films of different materials using FIB. The gas molecules will be adsorbed by the surface of the sample and will react with the incoming ions. The molecules decomposed by ion bombardment are desorbed from the surface leaving desired material atoms and forming a thin film on the surface. By controlling energy and current of the ion beam one can achieve a deposition to milling ratio which allows final thin films with thicknesses of several hundreds of nanometers. The films composition depends mainly in the gases available.

Since having been introduced to the field of metamaterials, FIB milling of nanomembranes for nanomechanical photonic metamaterials is proliferating. A huge range of designs and architectures can be envisioned through the usage of such versatile and powerful technology achieving the resolution needed to target optical wavelengths. Limitations arise from the time needed to fabricate larger metadevices, materials to be milled or ion species implantation. Nowadays, despite the increased difficulty to do so, also non conductive materials can be structured using FIB. Considering the different available ion sources and system configurations, the availability in terms of materials to be structured as metamaterials is immense. The advantages of high resolution, diversity of shapes and dimensions that can be obtained and the wide range of materials that can be milled/deposited outweigh the disadvantages of slow nanofabrication and high cost. FIB milling and deposition has already contributed hugely to advances in metamaterials and it is turning into a crucial technology for targeting smaller and smaller wavelengths [35, 59, 60]. Ideally, unit cell structuring for optical wavelength metamaterials can be developed and tuneability of reconfigurable planar photonic metamaterials brought to another stage of development.

3.2. Other Techniques

Producing metadevices for real world application will require great developments in nanofabrication. Focused ion beam is very powerful when it comes to prototyping, allowing to achieve proof-of-concept devices, however, when it comes to scale up processes, other solutions must be developed. Electron beam lithography has been widely developed in the last years as a way to overcome resolution limitations in traditional optical lithography. Electron beam lithography (EBL) consists of writing small patterns with an tightly focused electron beam in a radiation sensitive film, called a resist. A typical electron beam system mainly comprises an electron gun, a column, a chamber and a stage. The operation principles are very similar to the FIB, a high voltage allows extraction of electrons from a source and then accelerates, focus and align these electrons - along the column - until it reaches the sample to be patterned. In order to obtain high resolution nanostructures, sharp features and smooth surface several parameters must be optimized in the EBL system, such has electron energy densities, dwell times, sequence of exposure. These patterns are then developed in some chemical which selectively removes either the exposed or unexposed resist (positive- or negative- tone resist respectively). As for the FIB, the currents available can vary by changing the electron beam diameter and therefore the current density of the beam. Also a beam blanker is present to avoid exposure of unwanted areas.

The EBL tool can be available with two scan mechanisms of the electron beam, either raster or vector scan. Raster scan systems scan the beam continually in a raster scan and blank/unblank the

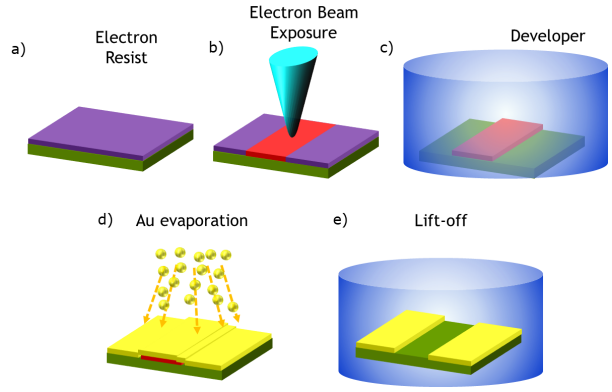

Figure 12. Schematic of the electron beam process combined with lift-off process Standard electron beam lithography in combination with lift-off process. a) Negative tone e-beam resist spin coating. b) E-beam exposure. c) Resist development, removing unexposed resist. d) Metal deposition. e) Metal lift-off covering the exposed resist remaining the patterned metal structure.

beam as appropriate to form the required pattern. Vector scan tools only scan the beam where it is actually required and tend to be slower but give smoother edges to the patterns. Figure 12 shows the overall e-beam lithography process. Firstly, a electron beam sensitive resist thin film is spun on the surface of a substrate (Figure 12a). The resist used and the conditions at which it is spun will result in completely different samples when it comes to the exposure process. Unlike photolithography and similarly to FIB, no mask is required to pattern a surface. Instead, the pattern data is handled by a computer which will control a finely focused beam of electrons and writes the desired pattern on the sample surface, see Figure 12b. When irradiated with electrons the solubility of the resist is altered causing a dissolution variation compared to areas that are not exposed. EBL typically uses 50 or 100 kV electron beams with diameters in the range 3 - 400 nm depending on the feature size required. For example, 100 kV electrons have a velocity of 0.57c which results in electron wavelenghts of around 4 pm. The exposure dose is an important parameter when patterning with electron beam, which is the required charge per unit area to expose the resist and is measured in $\mu C/cm^{-2}$. Typical values for 100 kV exposure are around 500 for a slow resist, eg PMMA, and 50 for a fast resist. As the dose per unit area decreases the tool has to scan the beam more rapidly. Optimizing exposure doses, currents and sequence for each system in question is crucial, since each resist and material will respond differently with the EBL system.

Next step is the development stage which is often simply a dip in a suitable developer, followed by a rinse and dry (Figure 12c). Finally, the pattern transfer stage converts the polymer resist pattern to something more useful - this can be either etching or deposition of certain layers. Upon patterning the resist layer with e-beam lithography, one must transfer this pattern to the substrate. This will be done by etching or deposition of the non-protected area. Wet etching, dry etching, ion milling, lift-off, thin film deposition or electrodeposition can be used alongside EBL processing. Figure 12 d and e, show the steps during the EBL nanostructuring using metal lift-off.

Overall, EBL is slow (comparable with FIB), is expensive (as it is FIB), can achieve great resolution, can provide great alignment for layer to layer (around 20 nm), specially if more complex processing is required (this is also possible with FIB) and the absence of a mask makes it a very flexible tool. While using FIB we only have to match the ion species to the material to be milled and optimize milling conditions, in order to achieve good yield and resolution, with EBL we also need to care about the etching/deposition process to be preformed afterward. EBL main advantage over the FIB is the better depth of focus which means it can be used to write, for instance, on the tops of pyramids. Using electron beam resists 10 nm minimum feature sizes can be achieved [61]. A common resist for sub-50 nm resolution is polymethylmetacrylate (PMMA) [62] while for highest resolution (below 20 nm) inorganic resists such as hydrogen silsesquioxane (HSQ) are also used [63]. Comparing to the FIB process, EBL is more complex since it needs more than just milling/exposure for the final pattern to be obtained. Often, resists spinning, baking, development and chemical baths must be used to achieve a final patter by EBL. Lately, development of EBL systems, allow researchers to fabricate fairly big areas at good speeds, achieving wafer fabrication in a couple of hours [64]. Combining EBL with FIB can delivery very promising on-chip nanomechanical photonic metamaterials [65]. In order to achieve such results, authors nanostructured individually addressable plasmonic chevron nanowires. The active structure of the metadevice has an effective area of 300 μm^2 and is fabricated by a combination of electron beam lithography and ion beam milling. In this case, metal lift-off is preformed after electron resist exposure and development. Such structures can act as spatial light modulator with sub-wavelength spatial resolution [44, 66] enabling tuneable gradient metamaterials, focusing elements or switchable diffraction gratings.

Also, by combining other techniques such as reactive ion etching, the development of ultrathin metamaterials consisting of a single 50 nm layer of free-standing gold can be achieved [59, 67, 68]. In order to achieve such ultrathin membranes of plasmonic metal

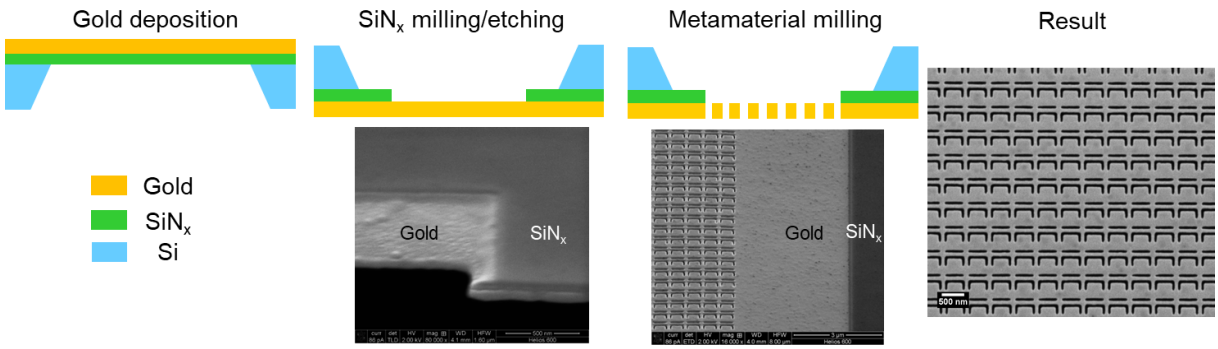

Figure 13. Fabrication steps for free-standing plasmonic membranes of deeply subwavelength thickness fabricated by focused ion beam milling. A metal film is deposited on a silicon nitride nanomembrane by resistive thermal evaporation. Subsequently, either FIB milling or etching can be used to remove the silicon nitride membrane layer. A symmetric, with respect to the light propagation direction, and deeply subwavelength free-standing membrane is obtained. Finally, FIB milling for structuring the free-standing layer into a metasurface is performed.

without supporting membrane , processes and methods that are not usually used in photonic metamaterials fabrication were brought into play. Dry etching mechanisms usually consist of sputtering materials with non-reactive gasses using high mass and energy in order to selectively remove material from a substrate. In [59, 67, 68], CHF_3 and Ar reactive ion etching is performed to completely remove the 50-nm-thick silicon nitride layer, see Figure 13. The previously deposited gold layer will not be affected. Due to the mostly vertical delivery of reactive ions, reactive-ion etching can produce very anisotropic etch profiles, which contrast with the typically isotropic profiles of wet chemical etching. By combining RIE process with FIB milling, authors realized free-standing gold membranes for fabrication of metasurfaces of deeply sub-wavelength thickness (typically 50 nm), with identical optical properties for different sides of light propagation.

High resolution nanostructures were already fabricated for nanomechanical photonic metamaterials. The techniques here mentioned are amongst the most important to the field. Targeting proof-of-concept prototyping, FIB and EBL systems stand out as the best solutions. It is interesting to think about which other processes from the nanoelectronic and nanophotonic fields can also be employed in combination with such powerful tools and what else can be achieved.

4. Applications and Future Perspective

Nanofabrication and nanomechanical photonic metamaterials are two fields that go hand-in-hand and are both relatively new. While nanofabrication has been carried out for decades, its optimization and full potential only now starts to be unlocked. As for the nanomechanical photonic metamaterials based on physical displacements, a lot of available forces have already been tested, however layering the device with different materials can increase versatility and open up opportunities. Improvements from both sides, nanofabrication and metamaterials design, can bring metadevices to real life applications and expand their wavelengths of operation, increase operation frequency and provide high contrast optical tuning. For example, improving resolution of the nanofabrication tools, smaller and smaller structures can be produced lowering the wavelength interaction (equation 8) for the metamaterials. Also, sharper features and closely packed metamolecules can improve tuneability and contrast (equation 9) due to stronger interactions and electric field enhancement.

The complexity of nanomechanical photonic metamaterials opens up several opportunities in very different realms. For instance, researchers have now computing power to model not only the electromagnetic response of a metamolecule but of an entire array. On top of that, mechanical models can be added to optimize nanomechanical photonic metamaterials design and simulate achievable displacements considering material properties and available forces. For example, designing unit cells with movable/addressable parts, can provide extremely fast tuneability since the structures are stiffer and therefore with higher frequency of operation, while smaller wavelength of interaction. Finally, nanofabrication process and final metadevices characteristics can also be modeled. These methods can provide good indications in which designs to pursue and which materials would result better for each applications. Some examples of nanostructures already realized and idealized for nanomechanical photonic metamaterials or fabricated using discussed methods in this tutorial are presented in Figure 14. From the overlook

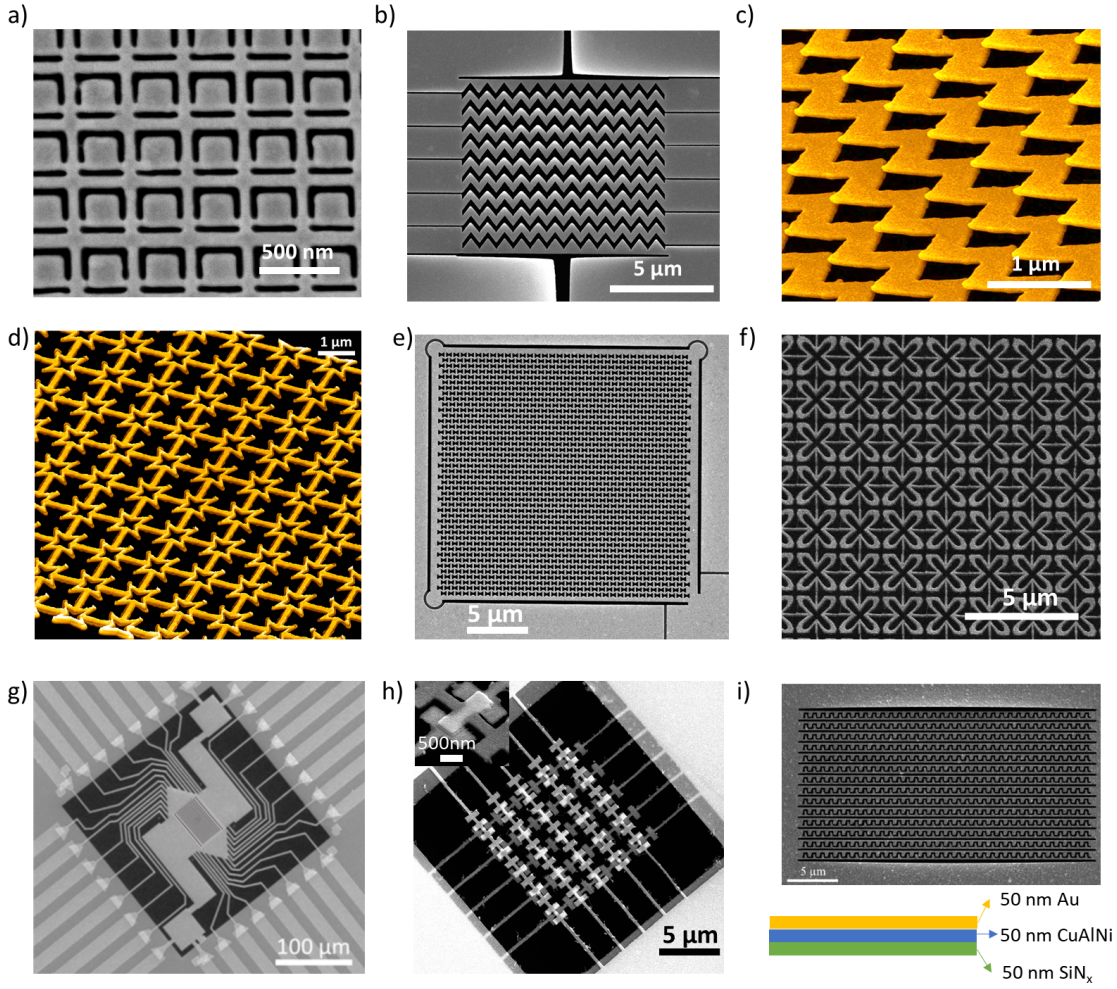

Figure 14. Opportunities for nanomechanical photonic metamaterials arising from the combination of FIB with other nanofabrication techniques a) Typical asymmetric split ring structures for coherent control experiments [59, 67–69] .b) Addressable gold photonic metamaterial and c) zoom up on the 50 nm thick gold bridges of metamaterials on b). All a), b) and c) are free-standing structures obtained on 50-60 nm thick gold layer after milling or etching of the silicon nitride membrane on the backside. d) e) and f) all represent different metamaterial structures fabricated on bilayer systems, 50 nm of gold and 50 nm of SiN_x These designs are all intended to combine mechanical and photonic metamaterial properties at the nanoscale [70]. g) Randomly addressable metamaterial fabricated by [65] using electron beam lithography combined with ion beam milling. h) Double side metamaterials where gold layer is structured by ion beam milling and silicon nitride membrane is etched away with reactive ion etching. The gold layer acts as a mask during the etching process. i) Shape memory alloy metamaterial. Combining different layers in the same metamaterials we can explore piezoelectric, shape memory alloys or phase change properties.

over the panels we can immediately acknowledge the diversity of structural designs that can be milled using FIB. Moreover ideas can be developed by milling and depositing materials while using the FIB or its combination with other techniques. From intricate shapes to single cuts through bilayer or monolayer systems, a lot has been fabricated and used in scientific experiments.

Figures 14a, b and c (row 1) show different gold plasmonic metamaterials of deeply sub-wavelength thickness that were fabricated by the same techniques. Either FIB milling or reactive ion etching of the silicon nitride membrane is used to achieve free-standing gold layers. Such layers are later nanostructured by FIB milling. Figures 14d, e, and f (row 2), shows the variety of designs developed in a bilayer (Au + SiN_x) for combination of mechanical and photonic metamaterials. The idea is that mechanical auxetic behaviour can be achieved at nanoscale and, at the same time, due to its dimensions, photonic metamaterial resonances are engaged [70]. Finally, the bottom row of Figure 14 illustrates opportunities

arising from the combination of nanofabrication processes and the introduction of novel functional materials. Authors have demonstrated on chip nanomechanical photonic metamaterials by combining EBL of a gold layer on a silicon nitride membrane to electrically address a FIB milled metamaterial on the bilayered area [65]. Also, in Figure 14h a double sided metamaterial is attempted, inspired by [14]. The same pattern was milled with FIB on different gold layers (one on each side of a silicon nitride membrane) and then reactive ion etching was preformed to remove the silicon nitride membrane. In the final example, a shape memory alloy layer (CuAlNi) was deposited between a plasmonic gold layer and a supporting silicon nitride membrane in order to explore its memory effect, see Figure 14i [71].

The challenge is to actuate only parts of a very small unit cell with the (weak) available forces. In order to address a 1 μm long cantilever the force needed is way stronger than estimated in this tutorial. However, if such small part of a unit cell can be addressed, extremely high frequency for very small wavelengths might be achieved. Another challenge for such small structures is to avoid switching of the structures. Since usually these metamaterials are irreversibly switched, avoiding different parts of the metamaterials to touch is crucial to avoid permanent damage (switching) of the structure. One of the ways to avoid this is to design metamolecules where the displacement movement instead of bringing parts of the metamolecules together will effectively separate them, for these, once more, highly accurate and sharp nanofabrication with improved resolution must be developed to start with extremely strong coupling (equation 9) and "'break it"' for tuning optical properties. Other materials might be brought into the reconfigurable photonic metamaterials platform in order to attain different optical properties, interact with other wavelengths or achieve different mechanical behaviours. Diamond, silicon or silicon oxide nanomembranes can act as mechanical support while transparent conductive oxides, graphene or alternative metallic layers can act as the plasmonic layer, for example. In fact, the combination of the above nanofabrication solutions with more standard CMOS fabrication techniques can allow us to develop different architectures and processes for nanomechanical photonic metamaterials. Moreover, different materials that act as mechanical support and plasmonic layer at the same time can also be brought into metadevice fabrication process. Piezoelectric materials [72] or other shape memory alloys [73] can be used in nanomechanical photonic metamaterials to achieve displacement and plasmonic response at the same time. Reducing metamolecules sizes will reach smaller wavelengths and provide tuneabilities at very high frequencies, provided that enough force can be available to engage displacement, not necessarily in and out of plane. Exploring new directions of movement or more complex displacements might be a way to achieve such goal. Either by careful design of the structures or by use of different materials (lower elastic restoring force), researchers aim to get smaller and faster. One concept being put forward is the coherent control of light, where the interaction between a standing wave and a planar metamaterial is altered by spatial manipulation (of the metamaterial) or standing wave manipulation (phase difference) [74]. This concept is being put forward on the tip of a optical fiber to manipulate light [75], at the same time, researchers envision using reconfigurable planar photonic metamaterials in the same way, allowing direct light manipulation in the media it propagates. Using reconfigurable planar photonic metamterials between optical fibers can bring great developments in optical computing, by enabling on fiber logic operations. Finally, several building blocks of nanophotonics can be put together to achieve superior performances. Nanowires could be combined with nanomechanical photonic metamaterials to fabricate tunable nanowire lasers, achieve on-chip tunable light sources, light channels and detectors. All of these could ultimately results in the development of optical on-chip computing.

5. Conclusions

This tutorial reflects on the key challenges in the field of nanomechanical photonic metamaterials while introducing different nanofabrication approaches and solutions to diversify it. Metamaterials have shown a huge number of tailored responses, however those responses are fixed by design and defined during nanofabrication. Regarding available forces to tune nanomechanical photonic metamaterials, a lot has been done and electrical currents, thermal changes, optical forces and magnetic fields have shown to be capable of driving reversible large-range tuning and modulation of metamaterial functionalities. Taking advantage of the versatility of nanomembrane technology structures have been actuated and optical properties tuned. Nanomechanical photonic metamaterials controlled by external stimuli have provided optical tuning and high frequency modulation of optical properties. Despite the experiments mentioned in this tutorial being mainly proof-of-principle demonstrations, each of them could be developed further and provide real world metadevices. Through an extensive and careful study of other possible designs, displacement directions (stretching or movement in plane) and

introducing materials used, there is still much room for optimization of responses and maximization of changes. Many other designs for dynamic control over phase, intensity and polarization of light can be envisioned. Practical and useful ways of achieving high frequency and high contrast tuning of metamaterial properties are based on electrostatic, electrothermal, magnetic or optical actuation. The Ampre force may also offer an opportunity to achieve small in plane displacements which can lead to large range tuning of metamaterial optical properties in a very efficient and simple way. Further optimization of actuators and optical resonators (design) can allow practical electrothermal or magnetoelectric light modulators and switches. Randomly addressable metamaterials that redirect, diffract, focus and modulate light on demand can be envisioned based on previously reported work. Moreover, taking nanofabrication technologies forward we can target the use of new materials, new layered designs and inclusion of active thin films on the nanomechanical photonic metamaterial structure. Also, merging of mechanical and electromagnetic metamaterials provides both a negative Poisson's ratio and resonant optical properties controlled by the metamaterial structure. These new interesting structures can enable nanomechanical metamaterials which keep their isotropy/anisotropy upon deformation. For this, practical solutions for actuation of auxetic metamaterials with a Poisson's ratio of approximately -1 will need to be developed.

Finally, this tutorial intends to provide an insight on novel and practical solutions for active control of metamaterials and the nanofabrication solutions that can be used. The results mentioned here, not only add to the rich electromagnetism of metamaterials, but also have contributed to bridging the gap between scientific proof-of-principle demonstrations and industrial applications of metamaterials. Potential applications range sub-wavelength resolution spatial light modulators and tuneable gradient metamaterials to focusing elements and magnetic field sensors.

6. References

[1] D. R. Smith, D. R. Smith, W. J. Padilla, W. J. Padilla, D. C. Vier, D. C. Vier, S. C. Nemat-Nasser, S. C. Nemat-Nasser, S. Schultz, and S. Schultz. "Composite Medium with Simultaneously Negative Permeability and Permittivity". *Physical Review Letters*, 84(18):4184–4187, 2000.

[2] R A Shelby, D R Smith, and S Schultz. "Experimental verification of a negative index of refraction". *Science*, 292(5514):77–79, 2001.

[3] V. A. Fedotov, P. L. Mladyonov, S. L. Prosvirnin, A. V. Rogacheva, Y. Chen, and N. I. Zheludev. "Asymmetric propagation of electromagnetic waves through a planar chiral structure". *Physical Review Letters*, 97(16):1–4, 2006.

[4] Xu Fang, Ming Lun Tseng, Jun Yu Ou, Kevin F. Macdonald, Din Ping Tsai, and Nikolay I. Zheludev. "Ultrafast all-optical switching via coherent modulation of metamaterial absorption". *Applied Physics Letters*, 104(14), 2014.

[5] Vyacheslav V Khardikov, Ekaterina O Iarko, and Sergey L Prosvirnin. "Trapping of light by metal arrays". *Journal of Optics*, 12(4):045102, 2010.

[6] A S Schwanecke, V A Fedotov, V V Khardikov, S L Prosvirnin, Y Chen, and N I Zheludev. "Optical magnetic mirrors". *Journal of Optics A: Pure and Applied Optics*, 9(1):L1–L2, 2007.

[7] U. Leonhardt. "Optical Confirmal Mapping". *Science*, 312:45221, 2006.

[8] Nikolay I. Zheludev and Yuri S. Kivshar. "From metamaterials to metadevices". *Nature Materials*, 11(11):917–924, 2012.

[9] N. Kida, Y. Kaneko, J. P. He, M. Matsubara, H. Sato, T. Arima, H. Akoh, and Y. Tokura. "Enhanced optical magnetoelectric effect in a patterned polar ferrimagnet". *Physical Review Letters*, 96(16):4–7, 2006.

[10] David A. Powell, Mikhail Lapine, Maxim V. Gorkunov, Ilya V. Shadrivov, and Yuri S. Kivshar. "Metamaterial tuning by manipulation of near-field interaction". *Physical Review B - Condensed Matter and Materials Physics*, 82(15):1–8, 2010.

[11] Christopher L. Holloway, Edward F. Kuester, Joshua A. Gordon, John O'Hara, Jim Booth, and David R. Smith. "An overview of the theory and applications of metasurfaces: The two-dimensional equivalents of metamaterials". *IEEE Antennas and Propagation Magazine*, 54(2):10–35, 2012.

[12] E. Ekmekci, A. C. Strikwerda, K. Fan, G. Keiser, X. Zhang, G. Turhan-Sayan, and R. D. Averitt. "Frequency tunable terahertz metamaterials using broadside coupled split-ring resonators". *Physical Review B - Condensed Matter and Materials Physics*, 83(19):4–7, 2011.

[13] G. R. Keiser, A. C. Strikwerda, K. Fan, V. Young, X. Zhang, and R. D. Averitt. "Decoupling crossover in asymmetric broadside coupled split-ring resonators at terahertz frequencies". *Physical Review B - Condensed Matter and Materials Physics*, 88(2), 2013.

[14] Xianliang Liu and Willie J. Padilla. "Dynamic Manipulation of Infrared Radiation with MEMS Metamaterials". *Advanced Optical Materials*, 1(8):559–562, 2013.

[15] Rutger Thijssen, Ewold Verhagen, Tobias J. Kippenberg, and Albert Polman. "Plasmon nanomechanical coupling for nanoscale transduction". *Nano Letters*, 13(7):3293–3297, 2013.

[16] Jeremiah P. Turpin, Jeremy A. Bossard, Kenneth L. Morgan, Douglas H. Werner, and Pingjuan L. Werner. "Reconfigurable and Tunable Metamaterials: A Review of the Theory and Applications". *International Journal of Antennas and Propagation*, 2014:1–18, 2014.

[17] Nanfang Yu, Patrice Genevet, Mikhail a Kats, Francesco Aieta, Jean-Philippe Tetienne, Federico Capasso, and Zeno Gaburro. "Light Propagation with Phase Discontinuities Reflection and Refraction". *Science*, 334(October):333–337, 2011.

[18] Eric Plum. *Chirality and Metamaterials*. PhD thesis, University of Southampton, 2010.

[19] C Balanis. *Advanced Engineering Electromagnetics*. Wiley, 1938.

[20] Ben Wood. "Structure and properties of electromagnetic metamaterials". *Laser and Photonics Reviews*, 1(3):249–259, 2007.

[21] J. D. Jackson. *Classical Electrodynamics*, volume 67. Wiley, 1999.

[22] J. Petschulat, C. Menzel, A. Chipouline, C. Rockstuhl, A. Tunnermann, F. Lederer, and T. Pertsch. "Multipole

approach to metamaterials". *Physical Review A - Atomic, Molecular, and Optical Physics*, 78(4):1–9, 2008.

[23] David J. Cho, Feng Wang, Xiang Zhang, and Y. Ron Shen. "Contribution of the electric quadrupole resonance in optical metamaterials". *Physical Review B - Condensed Matter and Materials Physics*, 78(12):1–4, 2008.

[24] Na Liu and Harald Giessen. "Coupling effects in optical metamaterials". *Angewandte Chemie - International Edition*, 49(51):9838–9852, 2010.

[25] J. Y. Ou, E. Plum, L. Jiang, and N. I. Zheludev. "Reconfigurable photonic metamaterials". *Nano Letters*, 11(5):2142–2144, 2011.

[26] Edward D. Palik. *Handbook of Optical Constants of Solids*, volume Ed.1. Academic Press, 1985.

[27] V. A. Fedotov, M. Rose, S. L. Prosvirnin, N. Papasimakis, and N. I. Zheludev. "Sharp trapped-mode resonances in planar metamaterials with a broken structural symmetry". *Physical Review Letters*, 99(14):5–8, 2007.

[28] Mikhail Lapine, Ilya V. Shadrivov, David A. Powell, and Yuri S. Kivshar. "Magnetoelastic metamaterials". *Nature Materials*, 11(1):30–33, 2011.

[29] Hu Tao, A. C. Strikwerda, K. Fan, W. J. Padilla, X. Zhang, and R. D. Averitt. "Reconfigurable terahertz metamaterials". *Physical Review Letters*, 103(14):1–4, 2009.

[30] Dmitry Chicherin. "MEMS-based high-impedance surfaces for milimeter and submilimeter wave aplpications". *Microwave and Optical Technology Letters*, 48(12):2781–2784, 2006.

[31] W M Zhu, A Q Liu, T Bourouina, D P Tsai, J H Teng, X H Zhang, G Q Lo, D L Kwong, and N I Zheludev. "Microelectromechanical Maltese-cross metamaterial with tunable terahertz anisotropy.". *Nature communications*, 3:1274, 2012.

[32] Yuan Hsing Fu, Ai Qun Liu, Wei Ming Zhu, Xu Ming Zhang, Din Ping Tsai, Jing Bo Zhang, Ting Mei, Ji Fang Tao, Hong Chen Guo, Xin Hai Zhang, Jing Hua Teng, Nikolay I. Zheludev, Guo Qiang Lo, and Dim Lee Kwong. "A micromachined reconfigurable metamaterial via reconfiguration of asymmetric split-ring resonators". *Advanced Functional Materials*, 21(18):3589–3594, 2011.

[33] Wei Ming Zhu, Ai Qun Liu, Xu Ming Zhang, Din Ping Tsai, Tarik Bourouina, Jing Hua Teng, Xin Hai Zhang, Hong Chen Guo, Hendrix Tanoto, Ting Mei, Guo Qiang Lo, and Dim Lee Kwong. "Switchable magnetic metamaterials using micromachining processes". *Advanced Materials*, 23(15):1792–1796, 2011.

[34] Jun-Yu Ou, Eric Plum, Jianfa Zhang, and Nikolay I Zheludev. "An electromechanically reconfigurable plasmonic metamaterial operating in the near-infrared.". *Nature nanotechnology*, 8(4):252–5, 2013.

[35] Joao Valente, Jun Yu Ou, Eric Plum, Ian J. Youngs, and Nikolay I. Zheludev. "Reconfiguring photonic metamaterials with currents and magnetic fields". *Applied Physics Letters*, 106(11), 2015.

[36] Jun Yu Ou, Eric Plum, Jianfa Zhang, and Nikolay I. Zheludev. "Giant Nonlinearity of an Optically Reconfigurable Plasmonic Metamaterial". *Advanced Materials*, 28(4):729–733, 2016.

[37] Nikolay I Zheludev and Eric Plum. "Reconfigurable nanomechanical photonic metamaterials". *Nat Nano*, 11(1):16–22, 2016.

[38] Srinivasan Prasanna and S. Mark Spearing. "Materials selection and design of microelectrothermal bimaterial actuators". *Journal of Microelectromechanical Systems*, 16(2):248–259, 2007.

[39] João Valente, Jun-Yu Ou, Eric Plum, Ian J. Youngs, and Nikolay I. Zheludev. "A magneto-electro-optical effect in a plasmonic nanowire material". *Nature Communications*, 6:7021, 2015.

[40] A. B. Munk. "Reflection Properties o f Periodic Surfaces o f Loaded Dipoles". *IEEE Transactions on Antennas and Propagation*, 19(5):612–617, 1971.

[41] Ronald L. Fante and Michael T. Mccormack. "Reflection Properties of the Salisbury Screen". *IEEE Transactions on Antennas and Propagation*, 36(10):1443–1454, 1988.

[42] Nader Enghetta. "Thin Absorbing Screens Using Metamaterial Surfaces". *Antennas and Propagation Society INternational Symposium*, 2:392–395, 2002.

[43] Pablo Cencillo-Abad, Jun-Yu Ou, Eric Plum, and Nikolay I. Zheludev. "Electro-mechanical light modulator based on controlling the interaction of light with a metasurface". *Scientific Reports*, 7(1):5405, 2017.

[44] Pablo Cencillo-Abad, Nikolay I. Zheludev, and Eric Plum. "Metadevice for intensity modulation with sub-wavelength spatial resolution". *Nature Publishing Group*, 6(November):1–7, 2016.

[45] Artemios Karvounis, Jun Yu Ou, Weiping Wu, Kevin F. Macdonald, and Nikolay I. Zheludev. "Nano-optomechanical nonlinear dielectric metamaterials". *Applied Physics Letters*, 107(19), 2015.

[46] Alexandra Boltasseva and Vladimir M. Shalaev. "Fabrication of optical negative-index metamaterials: Recent advances and outlook". *Metamaterials*, 2(1):1–17, 2008.

[47] M Soukoulis. "Past achievements and future challenges in the development of three-dimensional photonic metamaterials". *Nature Photonics*, pages 47–50, 2011.

[48] https://en.wikipedia.org/wiki/Skin_effect.

[49] H Wolferen, Leon Abelmann, and Henk van Wolferen. "Laser interference lithography". In *Lithography: Principles, Processes and Materials*, pages 133–148. Nova Science, 2011.

[50] Neilanjan Dutta, Iftekhar O. Mirza, Shouyuan Shi, and Dennis W. Prather. "Fabrication of large area fishnet optical metamaterial structures operational at near-IR wavelengths". *Materials*, 3(12):5283–5292, 2010.

[51] N. I. Zheludev, E. Plum, and V. A. Fedotov. "Metamaterial polarization spectral filter: Isolated transmission line at any prescribed wavelength". *Applied Physics Letters*, 99(17):1–4, 2011.

[52] I Bergmair, B Dastmalchi, M Bergmair, a Saeed, W Hilber, G Hesser, C Helgert, E Pshenay-Severin, T Pertsch, E B Kley, U Hübner, N H Shen, R Penciu, M Kafesaki, C M Soukoulis, K Hingerl, M Muehlberger, and R Schoeftner. "Single and multilayer metamaterials fabricated by nanoimprint lithography.". *Nanotechnology*, 22:325301, 2011.

[53] Steve Reyntjens and Robert Puers. "A review of focused ion beam applications in microsystem technology". *Journal of Micromechanics and Microengineering*, 11(4):287–300, 2001.

[54] J. Orloff. *Handbook of charged particle optics*. CRC Press, 2008.

[55] C. A. Volkert and A. M. Minor. "Focused Ion Beam Microscopy and Micromachining". *MRS Bulletin*, 32(05):389–399, 2007.

[56] Michael G. Stanford, Brett B. Lewis, Kyle Mahady, Jason D. Fowlkes, and Philip D. Rack. "Review Article: Advanced nanoscale patterning and material synthesis with gas field helium and neon ion beams". *Journal of Vacuum Science & Technology B, Nanotechnology and Microelectronics: Materials, Processing, Measurement, and Phenomena*, 35(3):030802, 2017.

[57] M Rosler. "Theory of Electron Emission from Solids by Proton and Electron Bombardment". *Phys. stat. sol. (b)*, 213:213–226, 1988.

[58] Michael G. Stanford, Kyle Mahady, Brett B. Lewis, Jason D. Fowlkes, Shida Tan, Richard Livengood, Gregory A. Magel, Thomas M. Moore, and Philip D.

Rack. “Laser-Assisted Focused He ⁺ Ion Beam Induced Etching with and without XeF ₂ Gas Assist”. *ACS Applied Materials & Interfaces*, 8(42):29155–29162, 2016.

[59] Thomas Roger, Stefano Vezzoli, Eliot Bolduc, Joao Valente, Julius J. F. Heitz, John Jeffers, Cesare Soci, Jonathan Leach, Christophe Couteau, Nikolay I. Zheludev, and Daniele Faccio. “Coherent perfect absorption in deeply subwavelength films in the single-photon regime”. *Nature Communications*, 6(May):7031, 2015.

[60] Venkatram Nalla, João Valente, Handong Sun, and Nikolay I. Zheludev. “11-Fs Dark Pulses Generated Via Coherent Absorption in Plasmonic Metamaterial”. *Optics Express*, 25(19):22620, 2017.

[61] P. Rai-Choudury. *Handbook of microlithography, micromachining and micro- fabrication: handbook of microlithography*, volume PM39. SPIE, 1997.

[62] Huigao Duan, Donald Winston, Joel K. W. Yang, Bryan M. Cord, Vitor R. Manfrinato, and Karl K. Berggren. “Sub-10-nm half-pitch electron-beam lithography by using poly(methyl methacrylate) as a negative resist”. *Journal of Vacuum Science & Technology B, Nanotechnology and Microelectronics: Materials, Processing, Measurement, and Phenomena*, 28(6):C6C58–C6C62, 2010.

[63] Vitor R. Manfrinato, Jianguo Wen, Lihua Zhang, Yujia Yang, Richard G. Hobbs, Bowen Baker, Dong Su, Dmitri Zakharov, Nestor J. Zaluzec, Dean J. Miller, Eric A. Stach, and Karl K. Berggren. “Determining the resolution limits of electron-beam lithography: Direct measurement of the point-spread function”. *Nano Letters*, 14(8):4406–4412, 2014.

[64] Raith. “EBL systems”.

[65] Pablo Cencillo-Abad, Jun-Yu Ou, Eric Plum, Joao Valente, and N.I. Zheludev. “Random access actuation of nanowire grid metamaterial”. *Nanotechnology*, 27(48):2–7, 2016.

[66] Pablo Cencillo-Abad, Eric Plum, Edward T F Rogers, and Nikolay I Zheludev. “Spatial optical phase-modulating metadevice with subwavelength pixelation”. *Opt. Express*, 24(16):18790–18798, 2016.

[67] Maria Papaioannou, João Valente, Eric Plum, and Nikolay I. Zheludev. “Two-dimensional control of light with light on metasurfaces”. *Light: Science & Applications*, 5:1–7, 2016.

[68] Maria Papaioannou, Eric Plum, João Valente, Edward T. F. Rogers, and Nikolay I. Zheludev. “All-optical multichannel logic based on coherent perfect absoprtion in a plasmonic metamaterial”. *APL Photonics*, 090801:1–9, 2016.

[69] Charles Michael Xavier Altuzarra, Stefano Vezzoli, Joao Valente, Weibo Gao, Cesare Soci, Daniele Faccio, and Christophe Couteau. “Coherent Perfect Absorption in Metamaterials with Entangled Photons”. *ACS Photonics*, page acsphotonics.7b00514, 2017.

[70] João Valente, Eric Plum, Ian J. Youngs, and Nikolay I. Zheludev. “Nano- and Micro-Auxetic Plasmonic Materials”. *Advanced Materials*, 28(26):5176–5180, 2016.

[71] Masanori Tsuruta, João Valente, Behrad Gholipour, Kevin F Macdonald, Eric Plum, and Nikolay I Zheludev. “Shape Memory Photonic Metamaterial”. *CLEO:2016 OSA 2016*, pages 3–4, 2016.

[72] Yu Hui, Juan Sebastian Gomez-Diaz, Zhenyun Qian, Andrea Alù, and Matteo Rinaldi. “Plasmonic piezoelectric nanomechanical resonator for spectrally selective infrared sensing”. *Nature Communications*, 7:1–9, 2016.

[73] Yusuke Nagasaki, Behrad Gholipour, Jun-Yu Ou, Masanori Tsuruta, Eric Plum, Kevin F. MacDonald, Junichi Takahara, and Nikolay I. Zheludev. “Optical bistability in shape-memory nanowire metamaterial array”. *Applied Physics Letters*, 113(2):021105, 2018.

[74] Eric Plum, Kevin F. MacDonald, Xu Fang, Daniele Faccio, and Nikolay I. Zheludev. “Controlling the Optical Response of 2D Matter in Standing Waves”. *ACS Photonics*, 4(12):3000–3011, 2017.

[75] Angelos Xomalis, Iosif Demirtzioglou, Eric Plum, Yongmin Jung, Venkatram Nalla, Cosimo Lacava, Kevin F. MacDonald, Periklis Petropoulos, David J. Richardson, and Nikolay I. Zheludev. “Fibre-optic metadevice for all-optical signal modulation based on coherent absorption”. *Nature Communications*, 9(1):1–7, 2018.

7. Acknowledgements

The author greatly acknowledges the companionship of everyone in the Optoelectronic Research Center and more specifically the Nanophotonics and Metamaterials group. This tutorial could not have been written without the help of J. Y. Ou, P. Cencillo-Abad, E. Plum and N. Zheludev, I thank them for their contributions. This work is supported by U.K.’s DSTL (Grant No. DSTLX1000064081) and the U.K.’s Engineering and Physical Sciences Research Council through the Nanostructured Photonic Metamaterials Programme Grant.

Competing financial interests: The authors declare no competing financial interests.